

## Effects of mechanical differences in sugarcane on the quality of mechanical harvesting

Zhi Li, Shiyan Li, Zhaoli Lin, and Hua Zhang\*

College of Agriculture National Engineering Research Center for Sugarcane, Fujian Agriculture and Forestry University, 350002, Fuzhou, China

Received July 4, 2022; accepted October 24, 2022

**Abstract.** The mechanization of the whole process of sugarcane harvesting is an integral part of reducing the cost of sugarcane production. In order to select sugarcane strains suitable for mechanized harvesting, in this experiment, a dynamic resistance strain gauge and other equipment determined the related mechanical property parameters such as density, elastic modulus, and Poisson's ratio of different sugarcane varieties. Ansys/explicit dynamics were used to establish a finite element model of the disc cutting device and to simulate the forces exerted on the stalk during sugarcane harvesting and also the quality of the cut section. Then, after obtaining the regression equation analysis and the response surface through the cross-section mass, the field harvesting experiment verifies the simulation results. The results show that the density, elastic modulus, and Poisson's ratio significantly affect the cutting quality within the three types of mechanical parameters. Through response surface analysis, when the elastic modulus is 92 MPa, the density is 1145 kg m<sup>-3</sup>, the Poisson's ratio is 0.404, the best cutting quality was obtained, and the section flatness is 57.09%. According to the cross-sectional regression equation, the calculation results are as follows: Liucheng 05-136 > Yuetang 94-128 > Guitang 42, which is the same as the actual harvest quality results under the two planting modes. This indicated that the difference in the mechanical properties of the sugarcane would significantly affect the quality of mechanical harvesting, which provides a reference direction for selecting sugarcane varieties suitable for mechanized harvesting.

**Keywords:** elastic modulus, Poisson's ratio, mechanized harvesting, finite element

### INTRODUCTION

The mechanized harvesting of sugarcane effectively reduces the cost of sugarcane production (Ou *et al.*, 2013). However, the quality of mechanical harvesting has become a bottleneck problem that is hindering further development, the cutting quality of basal cutting devices directly determines the production yield and disease resistance of ratoon sugarcane also plays a decisive role (Bachmann Schogor *et al.*, 2009; Damann, 1992). Therefore, improving the cutting quality and reducing the breakage rate of mechanized harvesting is imperative.

Researchers conducted research on the mechanized harvesting of crops using virtual simulation methods and conducted experiments on various crops. Liu *et al.* (2019) used finite element analysis to construct a cluster vibration simulation model based on the measurement of the tensile, compressive, shear, and bending properties of grapes. A virtual model was obtained of picking and cutting cluster picking at the end effector model and the corresponding cluster vibration and drop simulations were conducted for the picking process. Zhao *et al.* (2022) conducted a simulation study on the rice washing devices used in mechanized rice harvesting based on the DEM-CFD coupling method and analysed the effects of airflow speed and inclination angle on the washing effect. The results showed that the

increase in airflow velocity and inclination angle decreased the impurity rate of the rice and increased the entrainment loss rate. After tilting the screen surface by 10 degrees, combined with a force analysis of the particles on the screen surface, the results indicated an impurity rate and entrainment loss rate reduction in the rice. Qin *et al.* (2020) established a corn plant finite element model and its picking mechanism. The coupling effect of the three main factors; the rotating speed of the picking roller, the edge angle of the picking board and the feeding rate of the corn harvester were studied using a simulation. The results show that a picking roller running at a medium speed reduces the damage to the corn during the picking process and, at the same time, ensures a favourable harvesting efficiency, and also the optimal edge angle of the picking board is  $13^{\circ}\sim 15^{\circ}$ . Deng *et al.* (2021) used the finite element analysis method to study the collision characteristics of the steel bar with different parameters in a potato harvesting device, that is, the impact contact stress, the impact displacement, the acceleration, and the impact force. The results show that with increases in rod diameter, the maximum impact displacement of potato decreases, and the ultimate impact acceleration and impact peak force increase. The maximum crash displacement increases linearly, but the maximum crash acceleration and impact peak force decrease linearly with the rod inclination angle and rise in spacing. In order to improve the mechanized harvesting rate of olives. Hoshyarmanesh *et al.* (2017) simulated the effects of vibration frequency, loading type, temperature, and loading height on olive branch breakage. The results of the finite element modal analysis and field experiments were compared. The data were verified using a hydraulic eccentric mass dry shaker to obtain the required parameters and optimal efficiency for mechanized olive harvesting. Santos *et al.* (2015) developed a 3D finite element model to simulate the mechanical vibration picking process of coffee harvesting. The impact on the harvesting process of the inherent frequency of the coffee fruit stem, the pattern shape, and fruit maturity was analysed. This model is based on the linear elasticity theory and determines the stresses generated in the coffee cherries stem system through mechanical vibrations. The results showed that the natural frequency decreased with increasing fruit maturity. In addition, the as yet partially studied mechanized harvesting simulation for crops was also applied to crops such as chickpea (Golpira, 2013), banana (Guo *et al.*, 2021), and pepper (Kang *et al.*, 2020). Although the harvesting methods are slightly different in every case, simulation analysis has become essential in crop harvesting research.

The degree of maturity of the plant materials, moisture content and growth state all have partial effects on their mechanical strength. Li *et al.* (2022) analysed the relationship between the physical properties of rice grains and rice maturity. It was found that choosing the optimal harvest time of rice grains at maturity, that is, the point in

time at which the crop has an appropriate moisture content, can improve the yield of high-quality grains at the time of rice harvesting. Haman *et al.* (1994) analysed the effect of moisture content on the compressive capacity of rapeseed seeds. The Lamé equation was used to calculate the level of stress of rapeseed under compression. When the water content of the grain decreases, this could greatly improve the compressive stress. Dobrzański and Szot (1997) evaluated the effect of different moisture contents on the stress and strain of pea seed coats through performing a series of drying experiments. The pea seed coat tensile test results showed that an increase in moisture content was directly related to a decrease in the breaking force and obtained the same results for three pea varieties. Kalantari *et al.* (2022) combined image processing techniques with 3D modelling software for the volume estimation of irregular plant material. The estimated plant volume was compared with traditional mathematical expressions and actual volume measurements from the fluid displacement method to verify the rationality of the technique. Finally, a new physical property called the "cylindricity" factor was proposed, this determines that the plant material volume will also partially impact its mechanical properties. Jakob and Geyer (2021) analysed the removal force required for different cucumber varieties and in different years in the process of mechanical harvesting. It would inhibit the plant's growth if the average fruit removal force required for picking was too high. Only grasping and active disconnection can save both the plant and fruit from being damaged during the harvest. At the same time, the experimental results also showed a big difference in the ease of fruit removal among the different varieties, and this had nothing to do with the quality and length of the experimental samples. In summary, the part of the plant affected, its physiological condition, maturity stage, or moisture content will affect the deformation amplitude of the plant, this will ultimately affect the quality and yield of mechanical harvesting.

In the same time period, some researchers have performed a lot of research concerning mechanized sugarcane harvesting by various means. Araujo *et al.* (2021) analysed harvest quality and blade wear using digital image processing technology. The changes in leaf geometry (area, perimeter, rectangle, length) were assessed over time as were leaf wear and the harvest quality index (stalk damage index). This knowledge that was gathered could be applied to achieve better cut quality results during the mechanized harvesting process. Bahadori and Norris (2018) achieved the optimization of the operating parameters of Austoft 7000 harvester using sugarcane harvesting system (SCHLOT) software. The system was analysed on the basis of several factors, including the advance speed, rotation speed, harvest variety conditions, planting density, yield, harvest type, lodging status, and farm age. The aim was to optimize the results and minimize the harvest losses. Lai *et al.* (2011) established a mathematical model, and analysed the

effect of the stiffness of the sugarcane cutter on its working vibration and compared the ANSYS and ADAMS dynamic simulation analysis, the structural stiffness of the tool under two different simulation conditions. Physical experiments were performed to verify the actual effect of improving the tool stiffness. The results show that increasing rigidity of the cutter can significantly improve the standard of its sugarcane cutting quality. Hu *et al.* (2016) established geometric and finite element models to represent sugarcane. Stress-displacement diagrams and cutting force curves were obtained during a finite element analysis of the cutting process. The on-site cutting process of the tool was tested and verified. The results show that when the cutting disc speed is 600 rpm, the forward speed is  $0.5 \text{ m s}^{-1}$ , the blade edge angle is  $18^\circ$  and the cutting angle of the blade is  $20^\circ$  then the sugarcane breakage rate is minimized. Xing *et al.* (2021) conducted a series of simulation analyses on the extractor of a sugarcane harvester using the k-epsilon turbulence model to calculate the airflow distribution and the performance curve of the extractor at different impeller speeds. The results show that the rotational speed of the impeller only affects the wind speed of the airflow field. Improving the structure of the exhaust hood has the potential to avoid local eddy currents and the uneven distribution of airflow speed. Through the establishment of a sugarcane cutting dynamics model and virtual prototype simulation. Chen *et al.* (2018) discussed the influence of structural parameters such as the installation position and the lifting method of the cutting system on its dynamic characteristics. The results show that when the horizontal distance of the cutting system relative to the front wheel is 250 mm and the excitation frequency of the engine is 50 Hz, then lifting the cutting system and the entire frame minimizes

the amplitude of the tool. According to the research of Lv *et al.* (2008) the cutter continuously cuts multiple sugarcanes in the ANSYS and ADAMS kinematics module of the software and therefore the mechanism of each influencing factor was studied to determine its interaction with the head break rate. The results show a combination of a minor frequency and a low speed ratio. The low amplitude and the use of just a few blades are beneficial in reducing the breakage rate.

However, the overall progress of the research concerning the effect of the mechanical properties of sugarcane on cutting quality is insufficient. This study used a disc-type sugarcane harvesting device as a research object. A finite element method was used to study the effect of the different mechanical properties of sugarcane on the cutting quality. The combination of virtual testing and response surface analysis determined that the mechanical performance parameters of one group of sugarcane was most suitable for mechanized harvesting. At the same time, experiments were carried out concerning the field mechanized harvesting verification of sugarcane varieties with different mechanical properties in order to further illustrate the influence of the mechanical properties of sugarcane on its cutting quality. Finally, a sugarcane variety performance evaluation index suitable for mechanized harvesting was established, and the results could potentially help with the selection of excellent germplasm for mechanized harvesting.

## MATERIALS AND METHODS

AutoCAD (Autodesk, Inc. American) and GraphPad Prism (GraphPad Software, Inc. American) were used to produce the illustrations and process the data of this study.

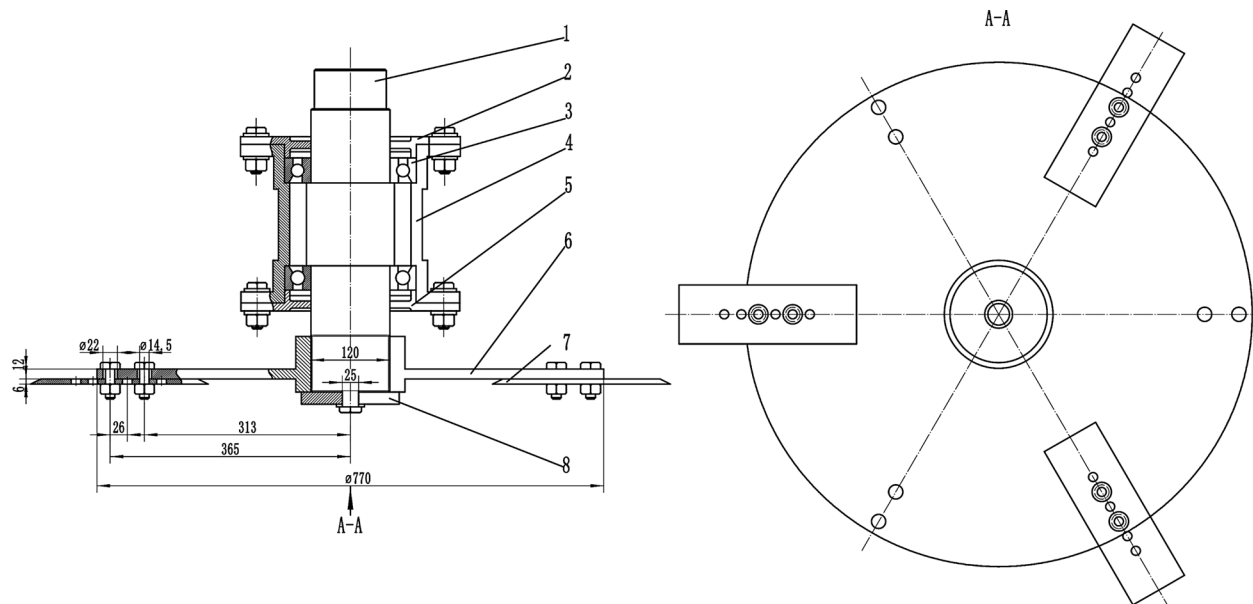


**Fig. 1.** The overall structure of the cutting device. 1– cutter shaft, 2– upper bearing end cover, 3 – bearing, 4 – sleeve, 5 – lower bearing end cover, 6 – cutter disc, 7 – blade, 8 – shaft end retaining ring.

The overall design of the structure of the cutting device is based on the physical and mechanical properties of the sugarcane stalk and the particular design of the disc cutting device, as shown in Fig. 1. The main parts of the machine include a cutter disc, blade, bearing end cover, cutter shaft, fixed sleeve, bearing, shaft end ring, *etc.* (Hou *et al.*, 2020). The bearings are embedded in the bushings. The cutter shaft passes through the sleeve, and one end of the shaft is matched with a transmission gear to transmit power to the cutter shaft. The bottom of the cutter shaft is connected to the cutter disc through a key and a shaft end retaining ring. This connection method provides torque to the cutter disc and ensures the stability of power transmission. At the same time, in order to facilitate the replacement of the blade, the blade and the cutter head are connected by bolts.

The first step is to determine the basic parameters of the operation. The forward speed is  $1 \text{ m s}^{-1}$ , and the rotation speed of the cutter disc is 480 rpm (Yang *et al.*, 2017). The diameter of the sugarcane stem is set to 28 mm. When the blade cuts into the sugarcane stem, a synergistic relationship occurs between the two. Figure 2 shows a diagram of the forces which occur when the cutter cuts evenly into the sugarcane stalk. According to the force analysis:

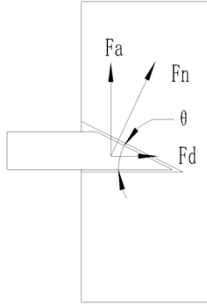


**Fig. 2.** Force diagram of sugarcane stalk.

$$F_d = F_n \sin \theta, \quad (1)$$

$$F_a = F_n \cos \theta, \quad (2)$$

where:  $F_d$  – diameter force generated during cutting (N),  $F_n$  – cutting force generated by the insert surface (N),  $\theta$  – tool edge inclination angle ( $^\circ$ ),  $F_a$  – axial force generated during cutting (N).

According to formulas (1)-(2), when the blade inclination  $\theta$  increases, the potential energy  $F_d$  required in the sugarcane cutting process will also increase, which in turn will increase the energy loss in the cutting process. Therefore, selecting the appropriate blade inclination angle is an essential means of reducing power consumption. The design should reduce the angle of  $\theta$  as much as possible. But when  $\theta$  is too small, the tool reduces the overall stiffness, increases blade wear, and greatly shortens the lifespan of the blade. At the same time, a smaller  $\theta$  will increase the manufacturing cost of the blade manufacturing process. Therefore, in considering the maximum benefit, the initial cutting blade inclination angle is  $20^\circ$ . Three blades were

installed on the cutter disc (Wang *et al.*, 2021). In order to improve the forward operation after cutting, an  $18^\circ$  inclination angle was maintained between the cutter head and the ground concurrently (Wang *et al.*, 2020).

When cutting stalks, combining different working parameters can cause the cutter to miss or overcut. Missing cuts can cause broken stalks through collisions with the horizontally advancing cutter disc, thereby increasing crop loss rates. Repeated cutting will increase the power consumption of the whole machine and the harvesting cost. Therefore, the maximum distance advanced  $S_{max}$  of the tool can be used as a reference for the effective working length. In determining the working length of the tool, the working cycle is generally defined in the following terms: when the centre point of the top edge of the second tool passes through the centre line of the first tool during the cutting process, the distance covered by the tool is the tool advance distance  $S$  (Fu *et al.*, 2018):

$$S = \frac{60v_m}{Zn}, \quad (3)$$

where:  $S$  – the effective length of the blade (mm),  $v_m$  – forward system speed, select  $400\text{-}2000 \text{ mm s}^{-1}$ ,  $Z$  – the number of blades, select 3,  $n$  – blade speed, select 480 rpm.

$$L = S_{max} + \Delta L, \quad (4)$$

where:  $L$  – tool working length (mm),  $S_{max}$  – the maximum distance advanced of the tool, according to formula (3),  $S_{max} = 83.3 \text{ mm}$ ,  $\Delta L$  – wear amount in the working direction, this varies according to the mechanical properties of the main stem of the sugarcane,  $\Delta L$  is taken as  $10\text{-}20 \text{ mm}$ .

According to the calculation, the working length of the tool is  $L = 95 \text{ mm}$ . In order to install the blade and cutter disc reliably, the experiment was designed to include six installation positioning holes with a diameter of  $14.5 \text{ mm}$ . The total length of the blade is  $270 \text{ mm}$ , and the total width is  $90 \text{ mm}$ , as shown in Fig. 3.

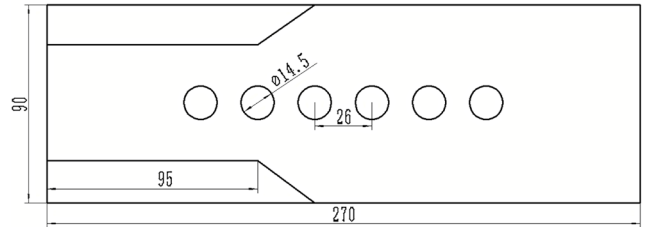


**Fig. 3.** Schematic diagram of the blade.

During the cutting process, the stem produces multiple stresses and deformations near the contact area with the cutter, which directly affects its cutting effect. In order to explore the influence of the different mechanical properties sugarcane on the cutting process, the cutting process of the disc cutter was simulated by applying ANSYS/explicit dynamics (Celik *et al.*, 2019).

Sugarcane stalk is a heterogeneous crop, which can be simplified to include cane stalks and cane nodes, and the whole is modelled as a solid cylinder (Qiu *et al.*, 2021).

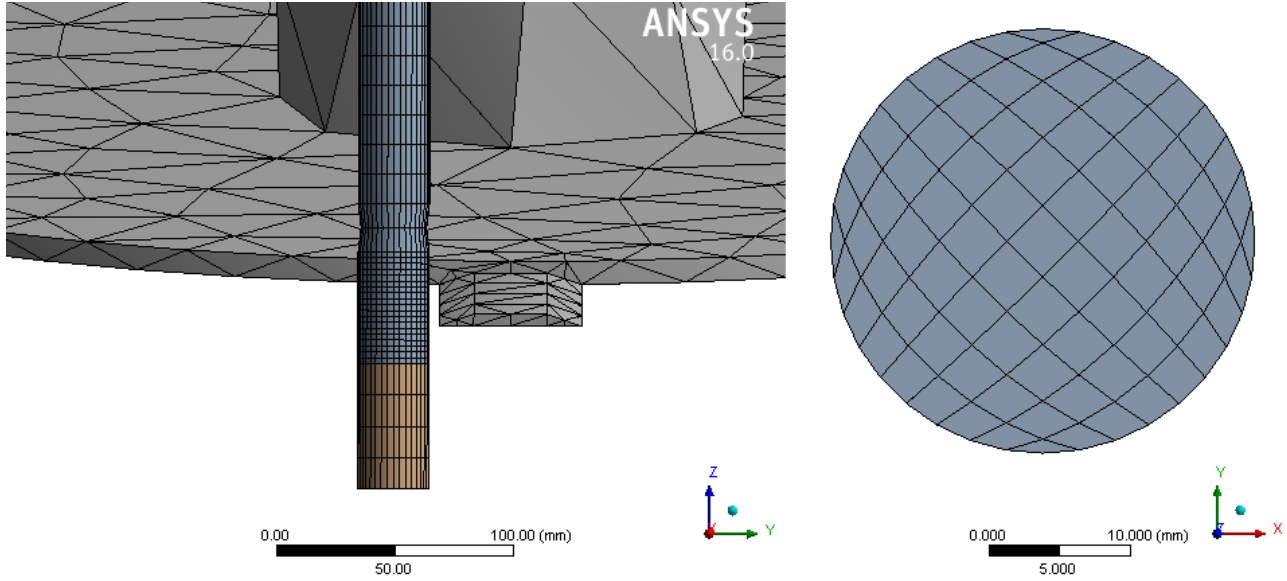


Fig. 4. Mesh division of the disc and sugarcane stalk.

The bolt hole of the blade is concentric with the cutter disc, and the bolt may be removed to use a fixed connection. Figure 4 shows the finite element model of the disc cutting sugarcane stalks.

In the finite element analysis process, the cutting system components such as the cutter disc and the blade are all made of homogeneous structural steel with a density of  $7850 \text{ kg m}^{-3}$ , a Poisson's ratio of 0.3, and an elastic modulus of  $2.11 \times 10^5 \text{ MPa}$  (Zuidema *et al.*, 1983).

Sugarcane stalk is an orthotropic linear elastic material due to its tissue structure. Assuming that a cubic sample is cut from the stalk, it has three symmetry axes of axial direction (L), diameter direction (R), and chord direction (T), that are approximately perpendicular to each other, and each of the axes forms a plane which may be referred to as TR, LR, LT respectively, there are three planes in all. The three axes considered can be modelled as mutually perpendicular elastic symmetry axes, and in this sense, sugarcane is an orthotropic material (Staab, 2015). Therefore, only nine independent parameters can be used to describe the sugarcane material under orthotropic conditions, namely  $E_L, E_R, E_T, \mu_{LR}, \mu_{LT}, \mu_{RT}, G_{LR}, G_{LT}, G_{RT}$ .

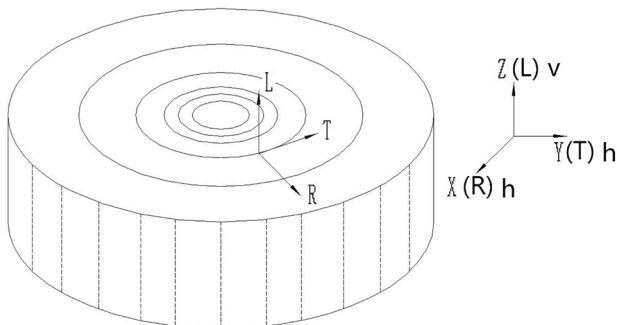


Fig. 5. Elastic main axis and the main elastic plane of sugarcane.

Further analysis of the sugarcane found that with each sublevel as the basic unit, individual nodes use internodes as transversely isotropic materials (Wang *et al.*, 2011). The stiffness coefficient and engineering elastic constant can be further transformed into elastic constants  $E_v, E_h, \mu_{vh}, \mu_{hh}, G_{hh}, G_{vh}$ .

Therefore, this study measured the dynamic elastic modulus of sugarcane through the application of the cantilever beam vibration method (Cao *et al.*, 2019). Range of values for Poisson's ratio and shear modulus  $E_v, E_h, \mu_{vh}, \mu_{hh}, G_{hh}, G_{vh}$  (Table 1).

In addition, density is also an essential mechanical evaluation index. As sugarcane matures, there is no significant difference in density among the different varieties. However, further analysis found that there were significant differences in the density of sugarcane during different growth stages, so the variable range of density may be defined as  $955\text{-}1145 \text{ kg m}^{-3}$ .

Therefore, the elastic constants mentioned above may be used as input for the ANSYS/explicit dynamics material module. The material property table of sugarcane is shown in Table 2.

According to the differemechanical properties of sugarcane stalks, there are a set of three material variables: density, axial elastic modulus, and axial Poisson's ratio, each with five levels. The results are shown in Table 3. In addition, the uniformly set material parameters in other directions in the ANSYS/explicit dynamics simulation were modelled according to Table 2.

Given the boundary conditions, a contact erosion algorithm between the cutter and the stalk (Huang *et al.*, 2011) was established. The static friction coefficient FS between the blade and the stalk is 0.3, and the dynamic friction coefficient FD is 0.2. The rotational speed of the central axis of

**Table 1.** Range of mechanical properties of sugarcane stalks

$E_v$	$E_h$	$\mu_{vh}$	$\mu_{vh}$	$G_{hh}$	$G_{vh}$
MPa				MPa	
0.384-0.897	92-126.9	0.386-0.462	0.223-0.252	0.153-0.317	31.45-45.76

**Table 2.** Sugarcane material property table in ANSYS/explicit dynamics material module

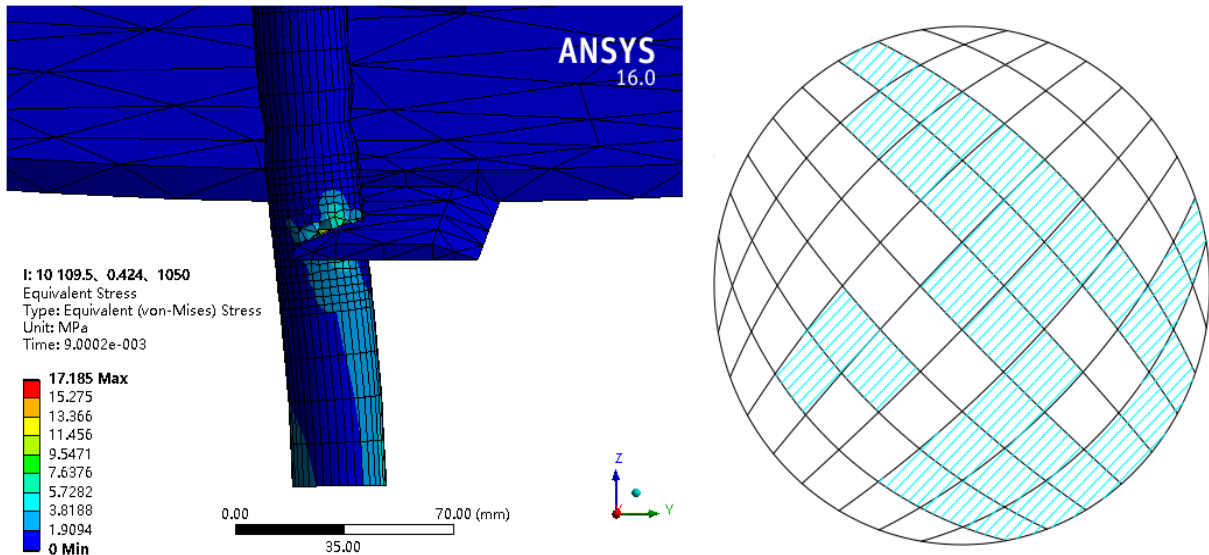
Density ( $\text{kg m}^{-3}$ )	$E_x$	$E_y$	$E_z$	$\mu_{xy}$	$\mu_{xz}$	$\mu_{yz}$	$G_{xy}$	$G_{xz}$	$G_{yz}$
	MPa						MPa		
955-1145	0.5	0.5	92-126.9	0.24	0.386-0.462	0.386-0.462	0.22	35	35

**Table 3.** Variable parameters of sugarcane stalk according to the mechanical level

Mechanical parameter	1	2	3	4	5
Axial modulus of elasticity (MPa)	80	92	109.5	127	139
Density ( $\text{kg m}^{-3}$ )	890	955	1050	1145	1210
Axial Poisson's ratio	0.36	0.386	0.424	0.462	0.488

**Table 4.** Dummy test factor coding table

Level	Factors		
	Elastic modulus (MPa)	Poisson's ratio	Density ( $\text{kg m}^{-3}$ )
Upper asterisk arm ( $\gamma$ )	138.9	0.488	1210
Upper level (1)	127	0.462	1145
Zero level (0)	109.5	0.424	1050
Lower level ( $-1$ )	92	0.386	955
Lower asterisk arm ( $-\gamma$ )	80.07	0.360	890.2
Distance change ( $\Delta j$ )	17.5	0.038	95

**Fig. 6.** Stalks stress and section flatness.

the cutter disc acts on all nodes of the cutter disc and the blade, and the fixed support constraint acts on one end of the sugarcane stalk.

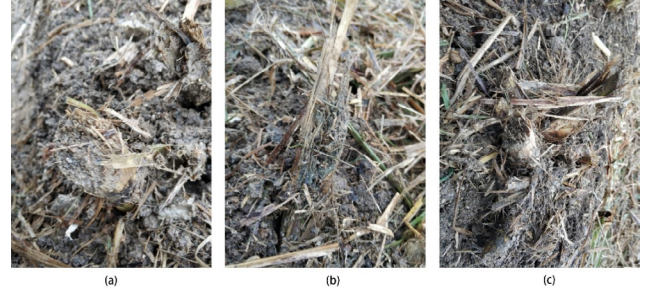
In order to study the cutting quality of sugarcane stalks under different mechanical performance parameters the flatness  $\eta$  of the sugarcane cutting plane was defined. The plane



**Table 5.** Simulation test results

Test number	Factors			Flatness (%)
	Elastic modulus (MPa)	Poisson's ratio	Density (kg m <sup>-3</sup> )	
1	92	0.386	955	52.77
2	127	0.386	955	38.83
3	92	0.462	955	48.83
4	127	0.462	955	17.3
5	92	0.386	1145	54.58
6	127	0.386	1145	46.75
7	92	0.462	1145	52.04
8	127	0.462	1145	19.83
9	80.07	0.424	1050	53.43
10	138.9	0.424	1050	26.14
11	109.5	0.360	1050	53.23
12	109.5	0.488	1050	23.83
13	109.5	0.424	890.2	46.46
14	109.5	0.424	1210	57.66
15	109.5	0.424	1050	45.02
16	109.5	0.424	1050	46.77
17	109.5	0.424	1050	44.01
18	109.5	0.424	1050	43.63
19	109.5	0.424	1050	47.15
20	109.5	0.424	1050	43.02

was divided into several small grids, and the ratio of the maximum flattened area to the total grid area of the region was defined. When  $\eta$  is closer to 1, the more smoothly the stalk is broken, and the better the cutting quality of the blade. The maximum area was obtained with the CAD area tool. The calculation method of estimating  $\eta$  is as follows:

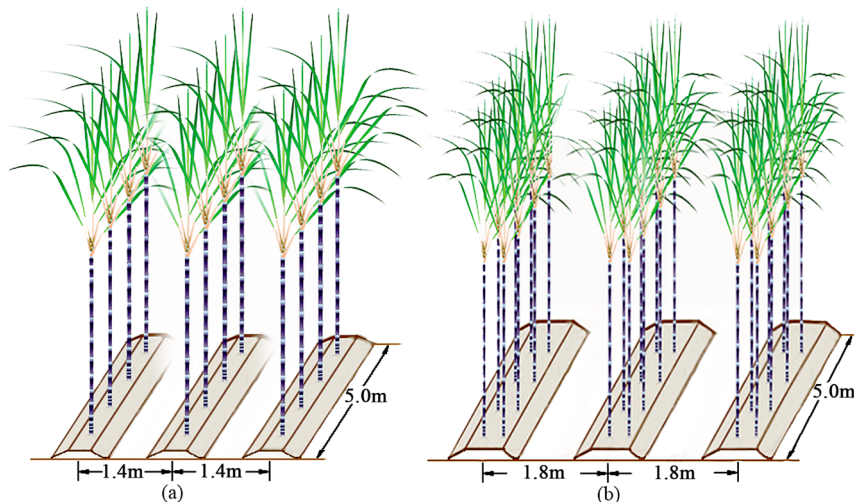
**Fig. 8.** Quality map of the on-site cutting section: a – levelling, b – stubble cutting, c – stubble removal.

$$\eta = \frac{s}{\pi D^2} 100, \quad (5)$$

where:  $\eta$  – stalk cut flatness (%),  $s$  – maximum flat area (mm<sup>2</sup>),  $D$  – stalk diameter (mm).

The required data was obtained using ANSYS/explicit dynamics software. A response surface analysis was performed using Design-Expert 12 test design software, the ternary quadratic general rotation combination method was used. The section flatness of the cut stalk was selected as the experimental evaluation index as well as the code design level of each factor, as shown in Table 4, the test results are shown in Table 5.

Three sugarcane varieties with different mechanical parameters were chosen to verify the simulation results: Guitang 42, Yuetang 94-128, and Liucheng 05-136. As shown in Figure 7, two planting modes were used for the mechanized harvesting operations and the cutting quality was evaluated by observing the cross-section after harvesting. Two planting modes of each variety were assessed in three experimental plots. Section quality was divided into three levels consisting of levelling, stubble breaking and stubble removal, as shown in Fig. 8, the experimental data was recorded.

**Fig. 7.** Planting pattern diagram: a – single row at 1.4 m interval, b – double row at 1.8 m interval.

## RESULTS AND ANALYSIS

Figure 9a refers to fixing the values of axial Poisson's ratio and axial elastic modulus. Under different density conditions, the sugarcane stalks behave in different ways when cut, with increases in density, the stress value first increases and then decreases, and the range of stress value is 15.02-18.17 MPa. By contrast, the section flatness first reduces and then increases. The variation range is 43.22-57.66%.

Figure 9b refers to fixing the axial Poisson's ratio and density values. Under the conditions of different axial elastic moduli that occur when the sugarcane stalk is cut, with increases in the elastic modulus the stress on the sugarcane stalk during the cutting process increases continuously, the values range from 13.24-29.46 MPa; the section flatness continues to decrease, and the variation range is 26.14-53.43%.

Figure 9c refers to fixing the axial elastic modulus and density values. Under different axial Poisson's ratios, the stress variation range of the sugarcane stalk cutting process is 14.30-25.18 MPa, while the flatness variation range is 23.83-54.24%.

Overall, there is a correlation between the stress value and flatness. That is, the change in the stress value determines the flatness of the section to a certain extent.

The resshow that when the cutter cuts the stalk, the minimum flatness of the cut section of the stalk is 17.3%, and the maximum surface flatness of the cut is 57.66%. A ternary quadratic regression equation was obtained by performing a regression analysis of the section flatness and experimental factors:

$$y = -384.22605 + 3.9703x_1 + 2385.47809x_2 - 0.4476434x_3 - 7.8891x_1x_2 + 0.0000408x_1x_3 - 0.138158x_2x_3 - 0.007323x_1^2 - 1860.47023x_2^2 + 0.000232x_3^2 \quad (6)$$

where:  $y$  – flatness (%),  $x_1$  – modulus of elasticity (MPa),  $x_2$  – Poisson's ratio,  $x_3$  – density ( $\text{kg m}^{-3}$ ).

In order to study the influence of the various test factors on the flatness of the sugarcane stalk section, the results were analysed for significance and variance. The results are shown in Table 6. The regression equation of sugarcane stalk section flatness was  $p < 0.01$ , and the regression model was highly significant. The missing item of  $p = 0.076 > 0.05$  indicated that the regression equation was well fitted and could be used to predict the influence of various factors on the surface flatness of the sugarcane stalk incision. According to the regression analysis, the order of influence of each factor on the quality of the stalk section was: Elastic modulus > Poisson's ratio > Density. In addition, the interaction of the elastic modulus and Poisson's ratio significantly affects the section quality. The regression equation may be simplified to:

$$y = -384.22605 + 3.9703x_1 + 2385.47809x_2 - 0.4476434x_3 - 7.8891x_1x_2 - 0.007323x_1^2 - 1860.47023x_2^2 + 0.000232x_3^2 \quad (7)$$

The adjusted R-Square  $R^2(\text{adj}) = 0.949 > 0.80$ , while the predicted  $R^2(\text{pre}) = 0.824$ , the difference between the two is less than 0.2, with good consistency. Adeq Precision determined a signal-to-noise ratio of  $20.68 > 4$ , and the ratio signal is sufficient thereby indicating that the model has sufficient resolution and can provide an appropriate reflection of the experimental results. At the same time, the coefficient of variation ( $\text{cv} = 6.28 < 15\%$ ), which reflects the absolute value of the degree of data dispersion within

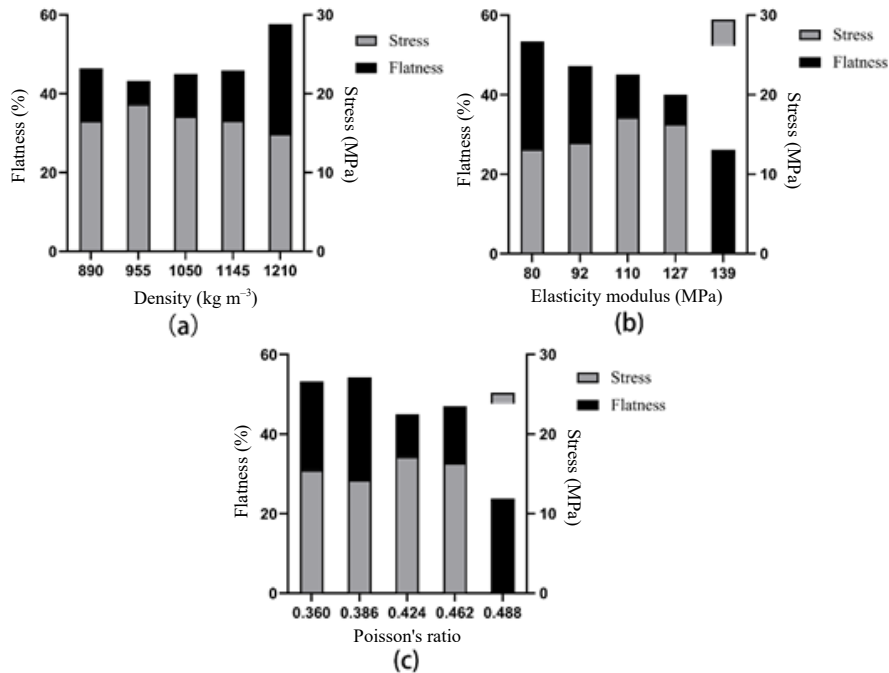
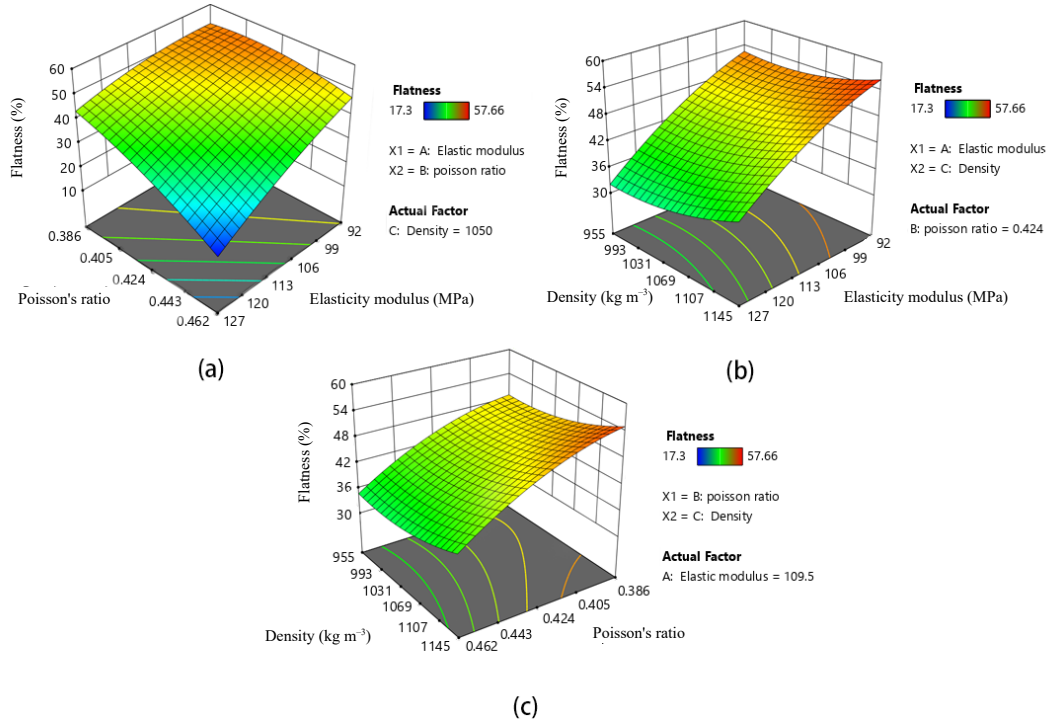


Fig. 9. Stress and flatness parameters: a – different density, b – different elasticity modulus, c – different Poisson's ratio.





**Fig. 10.** Influence of various factors on the flatness of the sugarcane cutting section: a – constant density, b – constant Poisson's ratio, c – constant elasticity modulus.

a reasonable range. In summary, this shows that the goodness of fit of the model is favourable. Its use indicates the influence of density, elastic modulus, and Poisson's ratio on cutting quality for preliminary analysis and prediction.

Each factor is a response to the surface effect results shown in Fig. 10. It may be observed in Fig. 10a that when the elastic modulus is in the range of 92-127 MPa, the flatness of the section caused by cutting decreases continuously with the increase in the elastic modulus. At the same time, when Poisson's ratio increases in the range of

0.386-0.462, the section flatness also shows a decreasing trend. Under the combined effects of the elastic modulus and Poisson's ratio, the section flatness assumes a minimum value at 127 MPa and 0.462.

It may be observed in Fig. 10b that when the density is between 955 and 1145 kg m<sup>-3</sup>, the flatness of the cutting section first decreases and then increases, but the change is not apparent. While the elastic modulus is 92-127 MPa, the section flatness still decreases significantly with the increase in the elastic modulus.

**Table 6.** Variance analysis of incision area simulation test results

Source	Sum of	df	Mean	F-value	p-value	
Model	2630	9	292.2	39.94	<0.0001	significant
A-E-Modulus	1264	1	1264	172.8	<0.0001	***
B-Poisson ratio	797.7	1	797.7	109.0	<0.0001	***
C-Density	86.18	1	86.18	11.78	0.0064	**
AB	220.2	1	220.2	30.10	0.0003	***
AC	3.69	1	3.69	0.504	0.4941	
BC	1.99	1	1.99	0.272	0.6133	
A2	72.49	1	72.49	9.91	0.0104	*
B2	104.0	1	104.0	14.22	0.0037	***
C2	63.38	1	63.38	8.66	0.0147	*
Residual	73.16	10	7.32			
Lack of fit	58.65	5	11.73	4.04	0.0757	not significant
Pure error	14.51	5	2.90			
Cor total	2703	19				

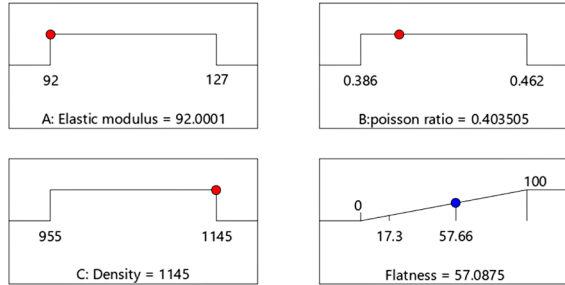


**Fig. 11.** Optimal predicted values of the influencing factor parameters. The red point represents the best value point of the factor, and the blue point represents the best result point.

**Table 7.** Theoretical section flatness of different sugarcane varieties

Variety	Elastic modulus (MPa)	Poisson's ratio	Density ( $\text{kg m}^{-3}$ )	Flatness (%)
Guitang 42	126.85	0.386	1084	46.25
Yuetang 94-128	99.11	0.432	1078	69.92
Liucheng 05-136	91.96	0.462	1052	74.60

Figure 10c shows that when Poisson's ratio is in the range of 0.386-0.462, the flatness of the sugarcane cutting section decreases significantly with the increase in Poisson's ratio. While the density is in the range of 955-1145  $\text{kg m}^{-3}$ , with increases in density, the section flatness still maintains the trend of first decreasing and then increasing, but the trend is still not obvious.

By taking the section flatness as the response value, Design Expert software was used to set the target value 'section flatness' as the maximum value. The maximum flatness

of the cut section of the sugarcane stalk was obtained as were the optimal predicted values of the parameters of each influencing factor. That is, when the elastic modulus is 92 MPa, the density is 1145  $\text{kg m}^{-3}$ , and the Poisson's ratio is 0.404, the section flatness is optimized, and reaches a maximum value of 57.09%. The section flatness value of 57.66% is close to the optimal parameter of the simulation. The results are shown in Fig. 11.

According to formula (7), the incision quality regression equation was used to calculate the theoretical section flatness of the three sugarcane varieties, the results are shown in Table 7.

The experimental verification results show that under the 1.8 m double-row planting mode, Liucheng 05-136 is 1.56-2.58%; the next is 2.08-3.68% of Yuetang 94-128, and Guitang 42. The stubble removal rate was 8.29-9.92%. In terms of the stubble breaking rate, the stubble breaking rates of Liucheng 05-136, Yuetang 94-128, and Guitang 42 are 46.91-48.44, 46.32-49.83, and 41.20-42.93%, respectively. In terms of the flat rate, the three values are: 49.78-50.52, 48.10-50.00, and 48.09-49.54%. Therefore, the cutting quality of Liucheng 05-136 is slightly better than that of Yuetang 94-128 and Guitang 42 under the double row spacing planting mode (Table 8), especially in terms of the stubble removal rate, Liucheng 05-136 < Yuetang 94-128 < Guitang 42.

The stubble removal rate of the analysis under the 1.4 m single-row planting mode, Liucheng 05-136 was 0.54-0.61%, while the stubble removal rate of Yuetang 94-128 and Guitang 42 were 1.02-1.64, and 0.60-2.42%. In terms of the stubble breaking rate, the stubble breaking rates of Liucheng 05-136, Yuetang 94-128, and Guitang 42 are 51.35-57.58, 48.73-56.06, and 49.76-56.21%, respectively.

**Table 8.** Variance analysis table of cutting quality difference among varieties

Cropping pattern	Section condition	Liucheng 05-136	Guitang 42	Yuetang 94-128
1.8 m wide row spacing double row	Stubble removal rate (%)	1.97±0.31b	9.15±0.47a	3.39±0.69b
	Levelling rate (%)	50.10±0.22a	48.80±0.42a	49.07±0.55a
1.4 m narrow line spacing single row	Stubble removal rate (%)	0.58±0.02a	1.54±0.53a	1.39±0.19a
	Levelling rate (%)	45.64±1.94a	46.29±1.55a	45.64±2.36a

Different lowercase letters after the numbers in the same row indicate significant differences at the 5% level. Data are means ± standard error.

**Table 9.** Variance analysis table of cutting quality difference between different planting patterns

Cropping pattern	Stubble removal rate (%)			Levelling rate (%)		
	Liucheng 05-136	Guitang 42	Yuetang 94-128	Liucheng 05-136	Guitang 42	Yuetang 94-128
1.8 m wide row spacing double row	1.97±0.31a	9.15±0.47a	3.39±0.69a	50.10±0.22a	48.80±0.42a	49.07±0.55a
1.4 m narrow line spacing single row	0.58±0.02b	1.54±0.53b	1.39±0.19b	45.64±1.94a	46.29±1.55a	45.64±2.36a

Different lowercase letters after the numbers in the same columns indicate significant differences at the 5% level. Data are means ± standard error.

In terms of the flat rate, the three values are: 41.82-48.11, 43.20-47.85, and 42.42-50.25%. From the analysis of the stubble rate, it is still Liucheng 05-136 < Yuetang 94-128 < Guitang 42.

At the same time, the cutting quality of the single-row planting mode is much better than that of the double-row planting mode (Table 9), and the single-row planting mode can control the stubble removal rate below 1%.

## DISCUSSION

According to the results shown in Fig. 9, the effect of cutting stress on the surface flatness of the cutting section is very significant. When a large amount of cutting stress is generated during the cutting process, it leads to more microstructure deformation, thereby generating a larger tensile stress in the cutting section (Chan *et al.*, 2011). It was found that cutting stress and section flatness are a pair of opposing parameters, and that a large degree of stress change will cause greater section damage.

The main reason for the variation in cutting stress is the difference in the mechanical properties of the different sugarcane varieties. The axial elastic modulus of the sugarcane is an important factor. A large elastic modulus can resist a greater degree of elastic deformation, and from a microscopic point of view, there is a greater bond strength between the atoms, ions, or molecules of the sugarcane (Guttman and Rothstein, 1979). The elastic modulus is the main cause of the difference in axial tensile stress of stalks also determines the material loss during the cutting process of sugarcane stalks.

However, a low elastic modulus will reduce the ability of sugarcane to resist external forces during the growth process, thereby making the sugarcane more prone to lodging (Yuan *et al.*, 2012), and reducing the sugar yield of sugarcane, and also increasing the difficulty of the mechanized harvesting process. Therefore, it is absolutely vital to choose the right variety of sugarcane.

Using the two-factor response surface plot, it was found that the interaction between the elastic modulus and Poisson's ratio has a significant effect on section flatness. However, both the interaction between the elastic modulus and density and the interaction between Poisson's ratio and density produced a weak impact on the section flatness. This is a slightly different situation from that in the single factor process, where the elastic modulus, Poisson's ratio and density all have significant effects on the section flatness. However, from an analysis of the whole model, the influence of the elastic modulus and Poisson's ratio on section flatness is extremely significant, while the influence of the density is significant. Seflek (2017) studied the elastic modulus and shear stress of stalks of 10 different maize varieties and found that there were significant differences between the physical properties of the stalks of the different varieties. In analysing the relationship between the elastic modulus and shear stress, it was found that a higher

elastic modulus corresponds to a larger shear stress, thereby indicating that stems with a high elastic modulus will require a greater shearing force during the cutting process. At the same time, the damage to the stem during the shearing process will also increase. This result is also consistent with our findings that a high elastic modulus can significantly reduce the flatness of the section. At the same time, Yilmaz *et al.* (2009) came to the same conclusion in a similar study conducted using sesame seeds. When analysing the physical and mechanical properties of unripe green grapes, Mirzabe and Hajiahmad (2021) found a correlation between the Poisson's ratio and the plant breaking force and firmness. When the Poisson's ratio gradually increased in the range of 0.4-0.48, the breaking force and hardness of the grapes gradually decreased. Analogous to the sugarcane cutting process, when the Poisson's ratio is gradually increased in the range of 0.4-0.48, the flatness of the cutting section is constantly decreasing. It is prone to damage and breakage, and it is not easy to maintain in an intact state. Through micro-mechanical research, Li *et al.* (2016) analysed the relationship between compressive stress and Poisson's ratio of tomato fruit cells by using the micro-extrusion method. It was found that Poisson's ratio had no significant effect on the compressive resistance of plants at the microscopic level. Dong *et al.* (2020) used X-ray tomography to detect characteristic parameters such as corn kernel density and porosity and stepwise regression was used to analyse the relationship between these characteristic parameters and the quality of maize mechanical harvesting. The results showed significant differences in the characteristic parameters of the grains of different maize varieties, and their effects on the crushing resistance of the maize grains were also significant. Therefore, the density of plant material is also an important factor that affects the quality of mechanized harvesting. In mechanized sugarcane harvesting, the use of high-density varieties can ensure a low porosity and less internal fracturing, which is necessary to maintain good section quality after harvest. This information may provide a better guide for optimal mechanized harvesting, the impact of the growth period is less important than the impact of the varieties used on harvest quality, which may in turn present a wide range of options concerning harvest times and varieties suitable for mechanized harvesting.

According to the field harvest data in Table 10, there are differences in harvest quality among the different varieties. Stubble removal reflects differences in harvest quality, these changes are irreversible in terms of sugarcane growth. A large stubble removal rate will significantly reduce the yield of ratoon sugarcane. According to the regression equation, the section flatness data obtained is Liucheng 05-136 > Yuetang 94-128 > Guitang 42. In the field of the cutting effect, the stubble removal rate reflects the same quality effect, that is, the stubble removal rate: Liucheng 05-136 < Yuetang 94-128 < Guitang 42. Therefore, it is emphasized that the differences in the mechanical properties of different sugarcane have an important impact on mechanized

**Table 10.** Field cutting conditions

Section condition	1.8 m wide row spacing double row									1.4 m narrow line spacing single row								
	Liucheng 05-136			Guitang 42			Yuetang 94-128			Liucheng 05-136			Guitang 42			Yuetang 94-128		
	area1	area2	area3	area1	area2	area3	area1	area2	area3	area1	area2	area3	area1	area2	area3	area1	area2	area3
Level / plant	98	112	96	63	107	100	95	111	139	78	69	89	73	89	99	81	84	99
Stubble break / plant	91	109	93	55	89	88	88	105	144	87	95	95	95	94	103	99	111	96
Stubble Removal / plant	5	4	3	13	20	17	7	10	6	1	1	1	1	3	5	3	3	2
Total / plant	194	225	192	131	216	205	190	226	289	166	165	185	169	186	207	183	198	197
Levelling rate (%)	50.52	49.78	50.00	48.09	49.54	48.78	50.00	49.12	48.10	46.99	41.82	48.11	43.20	47.85	47.83	44.26	42.42	50.25
Stubble break rate (%)	46.91	48.44	48.44	41.98	41.20	42.93	46.32	46.46	49.83	52.41	57.58	51.35	56.21	50.54	49.76	54.10	56.06	48.73
Stubble removal rate (%)	2.58	1.78	1.56	9.92	9.25	8.29	3.68	4.42	2.08	0.60	0.61	0.54	0.60	1.61	2.42	1.64	1.52	1.02

harvesting. That is, the impact of the varieties used on the quality of mechanized harvesting is significant. The same is true for other crops. Wang *et al.* (2020) harvested 42 maize varieties with the same mechanical parameters and analysed the breakage rate of the kernels during the mechanized harvesting of different varieties in order to obtain maize varieties suitable for mechanical harvesting. In order to screen rape varieties suitable for mechanized harvesting, Qing *et al.* (2021) conducted a field harvesting study on 15 varieties. It was found that compact, highly branched plant varieties had a better resistance to breakage. Moreover, varieties with a higher resistance to fruit drop and suitable plant traits for mechanized harvesting can significantly reduce field losses.

The difference in planting mode is also an essential factor affecting the harvest. Wang *et al.* (2019) studied the effects of different planting patterns of machine-picked cotton on cotton defoliation, yield, and fibre quality. The results showed that wide-row spacing and high-density planting could ensure a high yield without affecting fibre quality, and also promote early maturation, effectively reducing the impurity content of the machine-picked cotton and improving the quality of machine-picked cotton. The mechanized harvesting of regenerative rice technology has always been difficult in the case of rice. Zheng *et al.* (2022) adopted a skip-row planting approach in order to provide a path for the harvester and avoid crushing damage. Compared with the traditional model, the substantial decrease in planting density did not impact grain yield to any notable degree, it did not present an obstacle to effectively increasing the level of mechanical harvesting of regenerated rice. As with sugarcane, the stubble removal rate brought about by the single-row 1.4 m planting method is significantly lower than that of the double-row of 1.8 m. The three varieties examined in the study reflected

this result. This phenomenon may occur because double-row planting increases the difficulty of mechanized harvesting and places higher driving requirements on harvester drivers.

On the other hand, single-row planting is more conducive to soil cultivation during sugarcane production and provides better harvesting conditions for subsequent mechanized harvesting. At the same time, the lower cutting volume may produce less cutting vibration, which may also be the reason for the better harvest quality of the single-row planting mode. However, the single-row planting mode may produce a slightly lower yield than double-row planting, hence the need for a detailed grasp of the balance required in the planting process.

## CONCLUSIONS

After performing the research described above, the following concluding remarks may be presented:

1. The influence of the elastic modulus, Poisson's ratio, and density of sugarcane on the flatness of the cutting section may be expressed by a regression equation. That is, the influence of the various mechanical properties of sugarcane on the quality of mechanized harvesting is significant.

2. The maximum flatness of the sugarcane stalk cutting section and the optimal predicted values of the parameters of each influencing factor are as follows: the elastic modulus is 92 MPa, the density is 1145 kg m<sup>-3</sup>, the Poisson's ratio is 0.404, and the optimal value of the section flatness is 57.09%.

3. According to the section regression equation, the section flatness of the three sugarcane cutting theories is the same as the actual cutting effect. The cutting quality is Liucheng 05-136 > Yuetang 94-128 > Guitang 42. Also, an analysis of the field cutting process revealed that under the two planting modes, the mechanized harvest quality of single-row planting was significantly better than that of double-row planting.

**Conflicts of interest:** The authors declare no conflict of interest.

## REFERENCES

- Araujo G.D.M., Lima Dos Santos F.F., Hatum De Almeida S.L., Martins R.N., Voltarelli M.A., Strini Paixao C.S., and de Carvalho Pinto F.D.A., 2021.** Sugarcane harvesting quality by digital image processing. *Sugar Tech.*, 23, 209-218, <https://doi.org/10.1007/s12355-020-00867-2>
- Bachmann Schogor A.L., Nussio L.G., Mourao G.B., Muraro G.B., Sarturi J.O., and de Matos B.D.C., 2009.** Losses in sugarcane submitted to different harvesting methods. *Braz. J. Anim. Sci.*, 38, 1443-1450, <https://doi.org/10.1590/S1516-35982009000800007>
- Bahadori T. and Norris S., 2018.** Optimisation of farm management for reducing cane losses during mechanised sugarcane harvesting by using SCHLOT software model. *Int. Sugar J.*, 120, 462-464.
- Cao Y., Li M., Wang Z., Wang Y., and Gao Z., 2019.** Dynamic testing and analysis of Poisson's ratio of lumbers based on the cantilever-plate bending mode shape method. *J. Test. Eval.*, 47, 2540-2550, <https://doi.org/10.1520/JTE20160521>
- Celik H.K., Cinar R., Yilmaz D., Ulmeanu M., Rennie A.E.W., and Akinci I., 2019.** Mechanical collision simulation of potato tubers. *J. Food Process Eng.*, 42, 1-7, <https://doi.org/10.1111/jfpe.13078>
- Chan W., Fu M., and Lu J., 2011.** The size effect on micro deformation behaviour in micro-scale plastic deformation. *Mat. Des.*, 32, 198-206, <https://doi.org/10.1016/j.matdes.2010.06.011>
- Chen X., Tang L., Liu B., Lv L., Yang M., and Yang J., 2018.** Dynamic analysis and simulation of the cutting system of sugarcane harvester. *J. Chin. Agric. Mech.*, 39, 27-30, <https://doi.org/10.13733/jcam.issn.2095-5553.2018.05.006>
- Damann K., 1992.** Effect of sugarcane cultivar susceptibility on spread of ratoon stunting disease by the mechanical harvester. *Plant Disease*, 76, 1148-1149, <https://doi.org/10.1094/PD-76-1148>
- Deng W., Wang C., and Xie S., 2021.** Collision simulation of potato on rod separator. *Int. J. Food Engin.*, 17, 435-444, <https://doi.org/10.1515/ijfe-2020-0233>
- Dobrzański B. and Szot B., 1997.** Mechanical properties of pea seed coat. *Int. Agrophys.*, 11, 301-306.
- Dong P., Xie R., Wang K., Ming B., Hou P., Hou J., Xue J., Li C., and Li S., 2020.** Kernel crack characteristics for X-ray computed microtomography ( $\mu$ CT) and their relationship with the breakage rate of maize varieties. *J. Integr. Agric.*, 19, 2680-2689, [https://doi.org/10.1016/S2095-3119\(20\)63230-0](https://doi.org/10.1016/S2095-3119(20)63230-0)
- Fu Z., Wang D., Li W., Huang Y., and Zhu R., 2018.** Design and experiment of two-disc rotary mower of alfalfa. *Trans. Chin. Soc. Agric. Machin.*, 49, 214-220.
- Golpira H., 2013.** Conceptual design of a chickpea harvesting header. *Span. J. Agric. Res.*, 11, 635-641, <https://doi.org/10.5424/sjar/2013113-3728>
- Guo J., Karkee M., Yang Z., Fu H., Li J., Jiang Y., Jiang T., Liu E., and Duan J., 2021.** Research of simulation analysis and experimental optimization of banana de-handing device with self-adaptive profiling function. *Comput. Electron. Agric.*, 185, 2-24, <https://doi.org/10.1016/j.compag.2021.106148>
- Guttman L. and Rothstein J., 1979.** Computation of elastic-moduli from inter-atomic forces. *Phys. Rev. B.*, 19, 6062-6067, <https://doi.org/10.1103/PhysRevB.19.6062>
- Haman J., Dobrzański B., Szot B., and Stępniewski A., 1994.** Strength of shell in compression test of rapeseed. *Int. Agrophys.*, 8, 245-250.
- Hoshyarmanesh H., Dastgerdi H.R., Ghodsi M., Khandan R., and Zareinia K., 2017.** Numerical and experimental vibration analysis of olive tree for optimal mechanized harvesting efficiency and productivity. *Comput. Electron. Agric.*, 132, 34-48, <https://doi.org/10.1016/j.compag.2016.11.014>
- Hou J., Bai J., Yao E., and Zhu H., 2020.** Design and parameter optimization of disc type cutting device for castor stem. *IEEE Access.* 8, 191152-191162, <https://doi.org/10.1109/ACCESS.2020.3032535>
- Hu D., Zheng Y., and Zhao Y., 2016.** Movement simulation of sugarcane harvester cutter based on ANSYS/LS-DYNA. *Proc. 2016 Int. Conf. Engin. Sci. Manag. (ESM)*, 62, 268-271, <https://doi.org/10.2991/esm-16.2016.62>
- Huang H., Wang Y., Tang Y., Zhao F., and Kong X., 2011.** Finite element simulation of sugarcane cutting. *Editorial Office of Transactions of the Chinese Society of Agricultural Engineering*, 27, 161-166.
- Jakob M. and Geyer M., 2021.** Fruit removal forces of early stage pickling cucumbers for harvest automation. *Int. Agrophys.*, 35, 25-30, <https://doi.org/10.31545/intagr/131867>
- Kalantari D., Jafari H., Kaveh M., Szymanek M., Asghari A., Marczuk A., and Khalife E., 2022.** Development of a machine vision system for the determination of some of the physical properties of very irregular small biomaterials. *Int. Agrophys.*, 36, 27-35, <https://doi.org/10.31545/intagr/145920>
- Kang S., Kim J., Kim Y., Wooseungmin., Daniel D.U., and Ha Y., 2020.** A simulation study on the dynamics characteristics of hot pepper harvester. *J. Korea Soc. Simul.*, 29, 19-25, <https://doi.org/10.9709/JKSS.2020.29.3.019>
- Lai X., Li S., Ma F., Zhou J., and Zhang Z., 2011.** Dynamical analysis on sugarcane cutter rigidity enhancement. *Adv. Mech. Des.*, 199-200, 1387, <https://doi.org/10.4028/www.scientific.net/AMR.199-200.1387>
- Li Y., Chen Y., Ding Q., He R., and Ding W., 2022.** Analysis of relationship between head rice yield and breaking force of Japonica rice grains at different maturity stages. *Int. Agrophys.*, 36, 1-11, <https://doi.org/10.31545/intagr/145545>
- Li Z., Zhang Z., and Thomas C., 2016.** Viscoelastic-plastic behavior of single tomato mesocarp cells in high speed compression-holding tests. *Innov. Food Sci. Emerg. Technol.*, 34, 44-50, <https://doi.org/10.1016/j.ifset.2016.01.011>
- Liu J., Yuan Y., Gao Y., Tang S., and Li Z., 2019.** Virtual model of grip-and-cut picking for simulation of vibration and falling of grape clusters. *Trans. ASABE*, 62, 603-614, <https://doi.org/10.13031/trans.12875>
- Lv Y., Yang J., Liang Z., Mo J., and Qiao Y., 2008.** Simulative kinematics analysis on the affecting factors of rate of broken biennial root of single base cutter of sugarcane harvester. *Trans. Chin. Soc. Agric. Mach.*, 6, 50-55.
- Mirzabe A.H. and Hajiahmad A., 2021.** Physico-mechanical properties of unripe grape berries relevant in the design of juicing machine. *J. Food Process Engin.*, 44, 1-22, <https://doi.org/10.1111/jfpe.13859>
- Ou Y., Wegener M., Yang D., Liu Q., Zheng D., Wang M., and Liu H., 2013.** Mechanization technology: The key to sugarcane production in China. *Int. J. Agric. Biol. Engin.*, 6, 1-27, <https://doi.org/10.3965/ij.ijabe.20130601.001>



- Qing Y., Li Y., Xu L., and Ma Z., 2021.** Screen oilseed rape (*Brassica napus*) suitable for low-loss mechanized harvesting. *Agriculture-Basel*, 11, 1-13, <https://doi.org/10.3390/agriculture11060504>
- Qin J., Yin Y., Liu Z., Du Y., Wang G., Zhu Z., and Li Z., 2020.** Optimisation of maize picking mechanism by simulation analysis and high-speed video experiments. *Bios. Engin.*, 189, 84-98, <https://doi.org/10.1016/j.biosystemseng.2019.11.010>
- Qiu M., Meng Y., Li Y., and Shen X., 2021.** Sugarcane stem cut quality investigated by finite element simulation and experiment. *Bios. Engin.*, 206, 135-149, <https://doi.org/10.1016/j.biosystemseng.2021.03.013>
- Santos F.L., de Queiroz D.M., Magalhaes Valente D.S., and de Freitas Coelho A.L., 2015.** Simulation of the dynamic behavior of the coffee fruit-stem system using finite element method. *Acta Sci. Technol.*, 37, 11-17, <https://doi.org/10.4025/actascitechnol.v37i1.19814>
- Seflek A.Y., 2017.** Determining the physico-mechanical characteristics of maize stalks for designing harvester. *J. Anim. Plant Sci.*, 27, 855-860.
- Staab G.H., 2015.** 2 - A review of stress-strain and material behavior. In: *Laminar Composites* (Ed. G.H. Staab). Butterworth-Heinemann, 17-36, <https://doi.org/10.1016/B978-0-12-802400-3.00002-7>
- Wang F., Han H., Lin H., Chen B., Kong X., Ning X., Wang X., Yu Y., and Liu J., 2019.** Effects of planting patterns on yield, quality, and defoliation in machine-harvested cotton. *J. Integr. Agric.*, 18, 2019-2028, [https://doi.org/10.1016/S2095-3119\(19\)62604-3](https://doi.org/10.1016/S2095-3119(19)62604-3)
- Wang F., Ma S., Ke W., Xing H., and Bai J., 2020.** Energy consumption of sugarcane basecutting using contra-rotating basecutters. *Trans. ASABE*, 63, 317-324, <https://doi.org/10.13031/trans.13415>
- Wang F., Ma S., Ke W., Xing H., Bai J., Hu J., Yang Y., and Wei Y., 2021.** Optimization of basecutter structural parameters for under-the-ground sugarcane basecutting. *Appl. Engin. Agric.*, 37, 233-242, <https://doi.org/10.13031/aea.14178>
- Wang R., Zheng S., and Zheng Y., 2011.** Elementary mechanical properties of composite materials. In: *Polymer Matrix Composites and Technology* (Eds R. Wang, S. Zheng, and Y. Zheng). Woodhead Publishing, 357-548, <https://doi.org/10.1533/9780857092229.3.357>
- Wang Y., Li L., Gao S., Guo Y., Zhang G., Ming B., Xie R., Xue J., Hou P., Wang K., and Li S., 2020.** Evaluation of grain breakage sensitivity of maize varieties mechanically-harvested by combine harvester. *Int. J. Agric. Biol. Engin.*, 13, 8-16, <https://doi.org/10.25165/j.ijabe.20201305.6037>
- Xing H., Ma S., Wang F., Bai J., and Ma J., 2021.** Aerodynamic performance evaluation of sugarcane harvester extractor based on CFD. *Sugar Tech.*, 23, 627-633, <https://doi.org/10.1007/s12355-020-00920-0>
- Yang W., Wang E., Yang J., Li Y., Huang S., and Liang Z., 2017.** Test on influencing factors of cutting sugarcane quality of Case A8000 sugarcane combine harvester. *J. Agric. Mech. Res.*, 39, 192-196, <https://doi.org/10.13427/j.cnki.njyi.2017.05.037>
- Yilmaz D., Kabas O., Akinci I., and Cagirgan M.I., 2009.** Strength and deformation parameters of sesame stalk in relation to harvest. *Philipp. Agric. Sci.*, 92, 85-91.
- Yuan Z., Zhang X., Xu G., and Zhao X., 2012.** The influences of the stem structure and elastic modulus on wheat lodging. *Natur. Res. Sustain. Dev.*, 524-527, 2330-2333, <https://doi.org/10.4028/www.scientific.net/AMR.524-527.2330>
- Zhao L., Chen L., Yuan F., and Wang L., 2022.** Simulation study of rice cleaning based on DEM-CFD coupling method. *Processes*, <https://doi.org/10.28110.3390/pr10020281>
- Zheng C., Wang Y., Yuan S., Yu X., Yang G., Yang C., Yang D., Wang F., Huang J., and Peng S., 2022.** Effects of skip-row planting on grain yield and quality of mechanized ratoon rice. *Field Crops Res.*, 285, 1-11, <https://doi.org/10.1016/j.fcr.2022.108584>
- Zuidema J., Loopstra O., and Vansoest T., 1983.** The (pseudo) isotropic young modulus, rigidity modulus and poisson ratio of anisotropic rolled sheets. *Int. J. Mat. Res.*, 74(10), 643-651, <https://doi.org/10.1515/ijmr-1983-741003>